Acta Crystallographica Section C
Crystal Structure Communications
ISSN 0108-2701

Diaquadichloridobis(1*H*-imidazole)-manganese(II) at 100 K

Barbara Hachuła,[a]* Monika Pędras,[a] Danuta Pentak,[a] Maria Nowak,[b] Joachim Kusz[b] and Jerzy Borek[a]

[a]Institute of Chemistry, University of Silesia, 9 Szkolna Street, 40-006 Katowice, Poland, and [b]Institute of Physics, University of Silesia, 4 Uniwersytecka Street, 40-007 Katowice, Poland
Correspondence e-mail: bhachula@o2.pl

Received 25 February 2009
Accepted 23 April 2009
Online 2 May 2009

The mononuclear title complex, $[MnCl_2(C_3H_4N_2)_2(H_2O)_2]$, is located on a crystallographic inversion center. The Mn^{II} ion is coordinated by two imidazole ligands [Mn—N = 2.2080 (9) Å], two Cl atoms [Mn—Cl = 2.5747 (3) Å] and two water molecules [Mn—O = 2.2064 (8) Å]. These six monodentate ligands define an octahedron with almost ideal angles: the adjacent N—Mn—O, N—Mn—Cl and O—Mn—Cl angles are 90.56 (3), 92.04 (2) and 90.21 (2)°, respectively. Hydrogen bonds between the coordinated water molecules and Cl atoms form a two-dimensional network parallel to (100) involving $R_4^2(8)$ rings. The two-dimensional networks link into a three-dimensional framework through weaker N—H···Cl interactions. Thermogravimetric analysis results are in accordance with the water-coordinated character of the substance and its dehydration in two successive steps.

Comment

Imidazole (Im) is a structural element of many natural and/or synthetic organic compounds, including histidine and benzimidazole derivatives, exhibiting biological and pharmacological activities, such as antiviral (Cheng *et al.*, 2005), antifungal and antimycotic (Walter *et al.*, 1978), antihistaminic and antiallergic (Nakano *et al.*, 2000), antimicrobial (Sheng *et al.*, 2006), antihelminthic (Mavrova *et al.*, 2006), and antitumoral and antimetastatic properties (Charlston, 1973; Keppler *et al.*, 1987, 1989, 1993; Alessio *et al.*, 1993; Mestroni *et al.*, 1998; Mura *et al.*, 2001; Greiner *et al.*, 2007). The biological role of imidazole derivatives seems to be connected with the two N atoms with their different properties; the deprotonated N atom can coordinate with a metal ion, whereas the protonated N atom participates in hydrogen bonding (Santoro *et al.*, 1969; Reimann *et al.*, 1970; Ivarsson & Forsling, 1979; Lambert *et al.*, 2000; Shiu *et al.*, 2003; Masciocchi *et al.*, 2003; Huang *et al.*, 2004; Abuskhuna *et al.*, 2004; Gong *et al.*, 2005). These properties are used in different ways in proteins and enzymes that contain active sites with multiple histidine residues bound to a metal center, including carbonic anhydrase, nitrite reductase, dopamine β hydroxylase, superoxide dismutase, cytochrome *c* oxidase, pirin and acireductone dioxygenases (Greiner *et al.*, 2007).

The mononuclear title compound, (I) (Fig. 1), was obtained in an attempt to synthesize new Mn^{II} systems with imidazole derivative ligands. Despite its simplicity, no structural report of (I) was found in a search of the Cambridge Structural Database (CSD; Version 5.30 of November 2008; Allen, 2002). However, there were a few crystal structures of manganese(II) in which the ligands present were either only imidazole or a mixed imidazole/water system, *i.e.* $[Mn(Im)_6]Cl_2{\cdot}4H_2O$ (Garrett *et al.*, 1983*a*) and $[Mn(Im)_4(H_2O)_2]Cl_2$ (Garrett *et al.*, 1983*b*). The structures of the nickel(II) and cobalt(II) complexes analogous to (I), *viz.* $[CoCl_2(Im)_2(H_2O)_2]$ and $[NiCl_2(Im)_2(H_2O)_2]$, have already been reported (Atria *et al.*, 2003), but are not isostructural with (I).

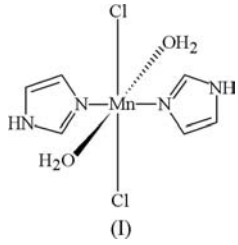

(I)

The Mn^{II} atom in (I) sits on a crystallographic center of inversion and is octahedrally coordinated by the monodentate ligands, *i.e.* two *N*-coordinated imidazole groups, two chloride anions and two O atoms of water molecules. The angles in the $[MnCl_2(Im)_2(H_2O)_2]$ octahedron are distorted by less than 2.1° from ideal values (Table 1).

The Mn1—N1 bond distance [2.2080 (9) Å] is slightly shorter than the average value in $[Mn(Im)_6]^{2+}$ (2.273 Å) and in other Mn complexes possessing imidazole ligands (Garrett *et al.*, 1983*b*; Krautscheid *et al.*, 1993; Liu *et al.*, 2001; Niu *et al.*, 2004; Kooijman, 2006; Lemoine *et al.*, 2006; Zhong *et al.*, 2006). The contraction of the latter bond is balanced by a lengthening of the Mn1—O1 bond [2.2064 (8) Å] when compared with the

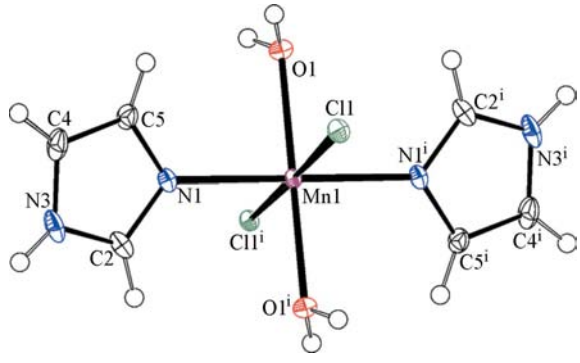

Figure 1
The asymmetric unit of (I), showing the atom-numbering scheme and 50% probability displacement ellipsoids. H atoms are shown as small spheres of arbitrary radii. [Symmetry code: (i) $-x+1, -y+1, -z$.]

 doi:10.1107/S0108270109015303

average value in $[Mn(H_2O)_6]^{2+}$ (2.177 Å; Carrell & Glusker, 1973). The Mn1—Cl1 distance [2.5747 (3) Å] is close to the value in $[MnCl_2(2\text{-MeIm})_3]$ (2.525 Å), in which one Cl atom is in an axial position (Phillips *et al.*, 1976). However, this Mn1—Cl1 length is different from that in $[MnCl_2(2\text{-MeIm})_3]$, which has the Cl atom in an equatorial position (2.392 Å; Phillips *et al.*, 1976). The coordinated imidazole rings of the title compound are essentially planar, with r.m.s. deviations from the mean plane of 0.0026 Å. The maximum deviation from the least-squares imidazole plane is observed for atom C2 [0.0032 (7) Å]. Atoms N1 and N3 are slightly out of the imidazole plane by −0.0015 (7) and −0.0036 (7) Å, respectively. The bond lengths in the coordinated imidazole ring are not significantly different from those in $[CoCl_2(Im)_2(H_2O)_2]$ and $[NiCl_2(Im)_2(H_2O)_2]$ (Atria *et al.*, 2003). The shortest bond is that between N1 and C2 [1.3184 (15) Å], while the longest bond, N1—C5 [1.3850 (15) Å], is located opposite. A common feature of the imidazole derivatives is the asymmetry of the two endocyclic N—C bonds; N1—C2 shows greater double-bond character than N3—C2 [1.3440 (17) Å]. The endocyclic angles of the aromatic ring differ somewhat from one another (see Table 1), namely in the closing of the angle at the atom to which the Mn atom is attached and the opening of the two adjacent angles.

The molecules are connected in the crystal lattice through intermolecular O1—H1O···Cl1^{ii} and O1—H2O···Cl1^{iii} hydrogen-bond interactions [symmetry codes: (ii) $-x+1, y-\frac{1}{2}, -z+\frac{1}{2}$; (iii) $x, -y+\frac{3}{2}, z+\frac{1}{2}$] and form eight-membered rings, with a graph-set motif of $R_4^2(8)$ (Etter *et al.*, 1990; Bernstein *et al.*, 1995), in the *bc* plane, leading to a two-dimensional network (see Fig. 2 and Table 2). Each water molecule bridges two $[MnCl_2(Im)_2(H_2O)_2]$ molecules. In turn, each $[MnCl_2(Im)_2(H_2O)_2]$ molecule is hydrogen bonded to four water molecules. Moreover, a weaker intermolecular hydrogen bond [N3—H3···Cl1^{iv}; symmetry code: (iv) $x+1, y, z$] joins the molecules into a three-dimensional network. Thus, each complex molecule possesses three potentially active H atoms (H3, H1O and H2O) involved in hydrogen bonds, with the Cl atom acting as the sole acceptor for all three interactions. Similar to the $[CoCl_2(Im)_2(H_2O)_2]$ and $[NiCl_2(Im)_2(H_2O)_2]$ complexes, the H···Cl distance in (I) between the coordinated imidazole group and coordinated Cl atom is slightly shorter than the sum of their van der Waals radii [2.515 (17) Å in (I), *cf.* 2.52 (17) Å (mean for 19 cases in the CSD; Atria *et al.*, 2003)]. In addition, the H···Cl bonds involving the aqua H atoms are slightly stronger than average [2.357 (19) and 2.367 (19) Å in (I), *cf.* 2.42 (18) Å (mean for 350 cases in the CSD; Atria *et al.*, 2003)]. The X-ray structure of (I) is similar to that of the previously reported Mn^{II} complex with the same ligands, $[Mn(Im)_4(H_2O)_2]Cl_2$, (II) (Garrett *et al.*, 1983*b*). Compound (II) crystallizes in the monoclinic *C*2/*c* space group and the Mn^{II} ion lies in an approximately octahedral coordination geometry completed by four N atoms and two coordinated water molecules. The adjacent $[Mn(Im)_4(H_2O)_2]^{2+}$ monomers are linked parallel to the *xy* plane into a three-dimensional metal–organic layer by hydrogen bonds between coordinated water molecules and interstitial chloride ions. Each chloride ion is also hydrogen bonded to two imidazole rings, one belonging to a complex in the same layer and the other belonging to a complex in an adjacent layer. The hydrogen-bonding interactions in (I) are shown in Fig. 2 and details are given in Table 2.

The FT–IR spectrum of $[MnCl_2(Im)_2(H_2O)_2]$ is in accordance with the X-ray crystallographic analysis and exhibits characteristic bands due to the functional groups of imidazole (Fig. 3). A strong and broad complex absorption between 3600 and 2000 cm^{-1} originates from the stretching of the hydrogen-bonded NH and OH groups in the compound. The sharp peak centered at 3282 cm^{-1} is attributed to ν_{O-H} of the water molecule. The narrow bands at 3151, 3133 and 3117 cm^{-1}, disturbing the ν_{N-H} band contour shape, correspond to the ν_{C-H} stretching modes of the imidazole ring. These frequencies are relatively close to the frequencies for pure imidazole

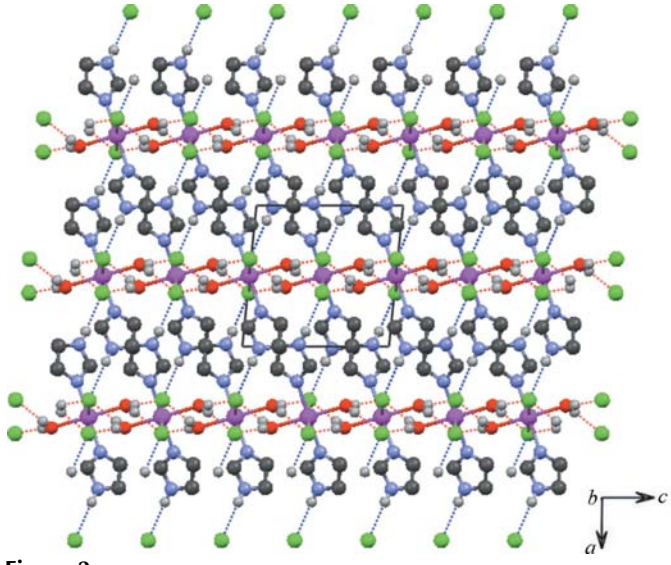

Figure 2
The packing in the crystal structure of $[MnCl_2(Im)_2(H_2O)_2]$, viewed along the *b* axis of the unit cell. The dashed lines (red and blue in the electronic version of the paper) indicate the hydrogen-bonding interactions (O1···Cl1 and N3···Cl1, respectively). For the sake of clarity, all H atoms bonded to C atoms have been omitted.

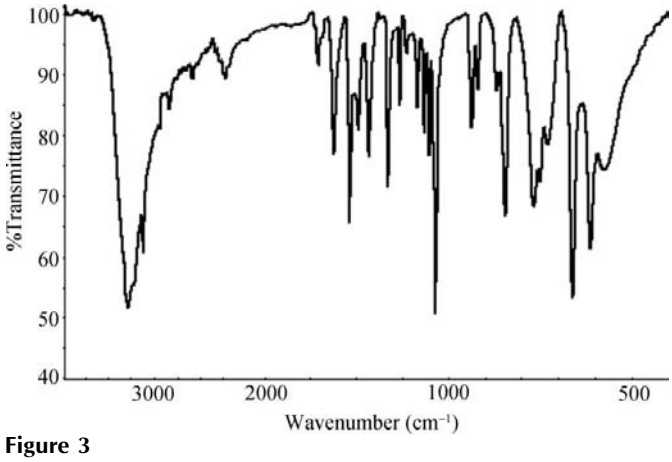

Figure 3
IR spectrum of a sample of (I) dispersed in a KBr pellet.

experimentally found by INS (3145, 3125 and 3120 cm^{-1}; Loeffen *et al.*, 1995). The band at 1622 cm^{-1} can be attributed to the stretching of the short Cl···HO bonds (Arif *et al.*, 2009). The vibrational bands from 1537 to 1070 cm^{-1} can be assigned to the ring stretching frequency of the imidazole ligand (Naumov *et al.*, 2001). The $\nu_{C=N}$ mode can be found at 1537 cm^{-1}. The bands remaining in the 937–729 cm^{-1} region can be associated with deformations of the imidazole ring. In the far IR region, a strong band at 661 cm^{-1} present in the complex is due to ν_{Mn-N} vibrations, and the peak at 578 cm^{-1} can be assigned to the bending vibration of the hydrogen bond (Arif *et al.*, 2009).

From the thermogravimetric analysis of (I) it results that there was a weight loss of about 86.95% in the temperature range 298–1173 K. The initial weight loss of 9.02%, occurring in two steps between 333 and 428 K, seems to be attributable to the removal of two solvent water molecules (calculated 12.09%). The next weight loss of 45.64% (calculated 45.69%) from 428 to 523 K corresponds to the removal of two imidazole molecules. Above 563 K, the release of Cl_2 occurs.

The electron paramagnetic resonance (EPR) spectrum of (I) in a powdered sample at room temperature shows only one isotropic signal at g = 2.00871, corresponding to manganese(II) in a weakly distorted octahedral environment, a geometry predicted by crystal structure analysis. Such an isotropic spectrum consisting of a broad signal without the hyperfine pattern is due to intermolecular dipole–dipole interactions and enhanced spin lattice relaxation (Garg *et al.*, 1998). When the manganese ion is magnetically diluted, the hyperfine interaction can be detected. The EPR spectrum of $[MnCl_2(Im)_2(H_2O)_2]$ in aqueous solution at 298 K exhibits a six-line manganese hyperfine pattern centered at g = 2.03068. These six hyperfine lines arise from the interaction of the electron spin with the nuclear spin (^{55}Mn, $I = \frac{5}{2}$) and correspond to $m_I = \pm\frac{5}{2}, \pm\frac{3}{2}$ and $\pm\frac{1}{2}$, resulting from allowed transitions ($\Delta m_s = \pm 1$, $\Delta m_I = 0$). The observed g values are close to the free electron spin value of 2.0023, suggestive of the absence of spin-orbit coupling in the ground state, $^6A_1$ (Sreekath *et al.*, 2006; Table 1).

Experimental

Hydrochloric acid (0.002 g, 0.05 mmol), manganese(II) chloride (0.126 g, 1 mmol) and imidazole (0.136 g, 2 mmol) were stirred in 2 ml of water until dissolved. The solution was filtered and the filtrate was left to stand undisturbed. After two days, colorless single crystals suitable for X-ray crystallographic analysis were collected and dried in air at room temperature. Elemental analysis calculated for $C_6H_{12}Cl_2MnN_4O_2$: C 24.18, N 18.79, H 4.06%; found: C 24.34, N 18.76, H 4.02%.

Crystal data

$[MnCl_2(C_3H_4N_2)_2(H_2O)_2]$
M_r = 298.04
Monoclinic, $P2_1/c$
a = 7.9364 (1) Å
b = 9.0864 (2) Å
c = 8.2480 (1) Å
β = 95.734 (2)°
V = 591.81 (2) Å^3
Z = 2
Mo $K\alpha$ radiation
μ = 1.55 mm^{-1}
T = 100 K
0.58 × 0.39 × 0.09 mm

Data collection

Oxford Diffraction Xcalibur diffractometer with a Sapphire3 CCD detector
Absorption correction: multi-scan (*CrysAlis RED*; Oxford Diffraction, 2008)
T_{min} = 0.532, T_{max} = 0.867
4794 measured reflections
1046 independent reflections
1017 reflections with $I > 2\sigma(I)$
R_{int} = 0.012

Refinement

$R[F^2 > 2\sigma(F^2)]$ = 0.014
$wR(F^2)$ = 0.038
S = 1.00
1046 reflections
82 parameters
H atoms treated by a mixture of independent and constrained refinement
$\Delta\rho_{max}$ = 0.23 e Å^{-3}
$\Delta\rho_{min}$ = −0.20 e Å^{-3}

Table 1
Selected geometric parameters (Å, °).

N3—C4	1.3672 (18)	C4—C5	1.3567 (17)
O1—Mn1—N1	90.56 (3)	C2—N3—C4	107.92 (10)
O1—Mn1—Cl1	90.21 (2)	N1—C2—N3	111.10 (11)
N1—Mn1—Cl1	92.04 (2)	C5—C4—N3	105.88 (11)
C2—N1—C5	105.49 (10)	C4—C5—N1	109.61 (11)

Table 2
Hydrogen-bond geometry (Å, °).

D—H···A	D—H	H···A	D···A	D—H···A
O1—H1O···Cl1^{ii}	0.816 (19)	2.357 (19)	3.1593 (9)	167.7 (16)
O1—H2O···Cl1^{iii}	0.815 (19)	2.367 (19)	3.1759 (9)	171.5 (16)
N3—H3···Cl1^{iv}	0.817 (17)	2.515 (17)	3.3231 (11)	170.1 (15)

Symmetry codes: (ii) $-x+1, y-\frac{1}{2}, -z+\frac{1}{2}$; (iii) $x, -y+\frac{3}{2}, z+\frac{1}{2}$; (iv) $x+1, y, z$.

C-bound H atoms were treated as riding on their parent C atoms [C—H = 0.95 Å and U_{iso}(H) = 1.2U_{eq}(C)]. H atoms that take part in hydrogen bonding were located in a difference Fourier map and refined freely with isotropic displacement parameters, with the exception that, for atom H3, the U_{iso}(H) value was fixed at 1.2U_{eq}(N).

Data collection: *CrysAlis CCD* (Oxford Diffraction, 2008); cell refinement: *CrysAlis RED* (Oxford Diffraction, 2008); data reduction: *CrysAlis RED*; program(s) used to solve structure: *SHELXS97* (Sheldrick, 2008); program(s) used to refine structure: *SHELXL97* (Sheldrick, 2008); molecular graphics: *ORTEP-3* (Farrugia, 1997) and *Mercury* (Macrae *et al.*, 2006); software used to prepare material for publication: *publCIF* (Westrip, 2009).

This research was supported by a scholarship from the UPGOW project co-financed by the European Social Fund.

Supplementary data for this paper are available from the IUCr electronic archives (Reference: SK3300). Services for accessing these data are described at the back of the journal.

References

Abuskhuna, S., McCann, M., Briody, J., Devereux, M. & McKee, V. (2004). *Polyhedron*, **23**, 1731–1737.
Alessio, E., Balducci, G., Lutman, A., Mestroni, G., Calligaris, M. & Attia, W. M. (1993). *Inorg. Chim. Acta*, **203**, 205–217.
Allen, F. H. (2002). *Acta Cryst.* B**58**, 380–388.
Arif, M., Nazir, S., Iqbal, M. S. & Anjum, S. (2009). *Inorg. Chim. Acta*, **362**, 1624–1628.

Atria, A. M., Cortés, P., Garland, M. T. & Baggio, R. (2003). *Acta Cryst.* C**59**, m396–m398.
Bernstein, J., Davies, R. E., Shimoni, L. & Chang, N.-L. (1995). *Angew. Chem. Int. Ed. Engl.* **34**, 1555–1573.
Carrell, H. L. & Glusker, J. P. (1973). *Acta Cryst.* B**29**, 638–640.
Charlston, A. J. (1973). *Carbohydr. Res.* **29**, 89–98.
Cheng, J., Xie, J. & Lou, X. (2005). *Bioorg. Med. Chem. Lett.* **15**, 267–269.
Etter, M. C., MacDonald, J. C. & Bernstein, J. (1990). *Acta Cryst.* B**46**, 256–262.
Farrugia, L. J. (1997). *J. Appl. Cryst.* **30**, 565.
Garg, B. S., Kurup, M. R. P., Jain, S. K. & Bhoon, Y. K. (1998). *Transition Met. Chem*. **13**, 92–95.
Garrett, T. P. J., Guss, J. M. & Freeman, H. C. (1983*a*). *Acta Cryst.* C**39**, 1027–1031.
Garrett, T. P. J., Guss, J. M. & Freeman, H. C. (1983*b*). *Acta Cryst.* C**39**, 1031–1034.
Gong, Y., Hu, C., Li, H., Pan, W., Niu, X. & Pu, Z. (2005). *J. Mol. Struct*. **740**, 153–158.
Greiner, B. A., Marshall, N. M., Narducci Sarjeant, A. A. & McLauchlan, C. C. (2007). *Inorg. Chim. Acta*, **360**, 3132–3140.
Huang, X. C., Zhang, J. P., Lin, Y. Y., Yu, X. L. & Chen, X. M. (2004). *Chem. Commun*. **9**, 1100–1101.
Ivarsson, G. J. M. & Forsling, W. (1979). *Acta Cryst.* B**35**, 1896–1897.
Keppler, B. K., Henn, M., Juhl, U. M., Berger, M. R., Niebl, R. & Wagner, F. E. (1989). *Prog. Clin. Biochem. Med*. **10**, 41–69.
Keppler, B. K., Lipponer, K. G., Stenzel, B. & Kratz, F. (1993). *Metal Complexes in Cancer Chemotherapy*, p. 187. Weinheim: VCH.
Keppler, B. K., Rupp, W., Juhl, U. M., Endres, H., Niebl, R. & Baizer, W. (1987). *Inorg. Chem.* **26**, 4366–4370.
Kooijman, H. (2006). *Acta Cryst.* E**62**, m2681–m2682.
Krautscheid, U., Dev, S., Krautscheid, H., Paul, P. P., Wilson, S. R. & Rauchfuss, T. B. (1993). *Z. Naturforsch. Teil B*, **48**, 653–658.
Lambert, F., Renault, J. P., Policar, C., Badarou, I. M. & Cesario, M. (2000). *Chem. Commun.* **1**, 35–36.
Lemoine, P., Viossat, V., Dayan, E., Dung, N.-H. & Viossat, B. (2006). *Inorg. Chim. Acta*, **359**, 4274–4280.
Liu, Y., Xu, D. & Liu, J. (2001). *J. Coord. Chem*. **54**, 175–781.
Loeffen, P. W., Pettifer, R. F., Fillaux, F. & Kearley, G. J. (1995). *J. Chem. Phys.* **103**, 8444–8455.
Macrae, C. F., Edgington, P. R., McCabe, P., Pidcock, E., Shields, G. P., Taylor, R., Towler, M. & van de Streek, J. (2006). *J. Appl. Cryst.* **39**, 453–457.
Masciocchi, N., Ardizzoia, G. A., Brenna, S., Castelli, F., Galli, S., Maspero, A. & Sironi, A. (2003). *Chem. Commun*. **16**, 2018–2019.
Mavrova, A. Ts., Anichina, K., Vuchev, D. I., Tsenov, J. A., Denkova, P. S., Kondeva, M. S. & Micheva, M. K. (2006). *Eur. J. Med*. **41**, 1412–1420.
Mestroni, G., Alessio, E., Sessanta o Santi, A. S., Geremia, S., Bergamo, A., Sava, G., Boccarelli, A., Schettino, A. & Coluccia, M. (1998). *Inorg. Chim. Acta*, **273**, 62–71.
Mura, P., Casini, A., Marcon, G. & Messori, L. (2001). *Inorg. Chim. Acta*, **312**, 74–80.
Nakano, H., Inoue, T., Kawasaki, N., Miyataka, H., Matsumoto, H., Taguchi, T., Inagaki, N., Nagai, H. & Satoh, T. (2000). *Bioorg. Med. Chem*. **8**, 373–380.
Naumov, P., Ristova, M., Soptrajanov, B. & Zugik, M. (2001). *J. Mol. Struct*. **598**, 235–243.
Niu, S.-Y., Zhang, S.-S., Li, X.-M., Wen, Y.-H. & Jiao, K. (2004). *Acta Cryst.* E**60**, m209–m211.
Oxford Diffraction (2008). *CrysAlis CCD* and *CrysAlis RED*. Oxford Diffraction Ltd, Wrocław, Poland.
Phillips, F. L., Shreeve, F. M. & Skapski, A. C. (1976). *Acta Cryst.* B**32**, 687–692.
Reimann, C. W., Santoro, A. & Mighell, A. D. (1970). *Acta Cryst.* B**26**, 521–526.
Santoro, A., Mighell, A. D., Zocchi, M. & Reimann, C. W. (1969). *Acta Cryst.* B**25**, 842–847.
Sheldrick, G. M. (2008). *Acta Cryst.* A**64**, 112–122.
Sheng, J., Nguyen, P. T. M., Baldeck, J. D., Olsson, J. & Marquis, R. E. (2006). *Arch. Oral Biol*. **51**, 1015–1023.
Shiu, K.-B., Yen, C.-H., Liao, F.-L. & Wang, S.-L. (2003). *Acta Cryst.* E**59**, m1189–m1191.
Sreekath, A., Joseph, M., Fun, H.-K. & Kurup, M. R. P. (2006). *Polyhedron*, **25**, 1408–1414.
Walter, K. A. M., Braemer, A. C., Hitt, S., Jones, R. E. & Matthews, T. R. (1978). *J. Med. Chem.* **21**, 840–843.
Westrip, S. P. (2009). *publCIF*. In preparation.
Zhong, C.-M., Zuo, Y.-J., Jin, H.-S., Wang, T.-C. & Liu, S.-Q. (2006). *Acta Cryst.* E**62**, m2605–m2606.